International Symposium
On Turbulence and Shear Flow
Phenomena (TSFP-9)
June 30 - July 3, 2015 *Melbourne, Australia*

FLOW CONTROL OVER SWEPT WINGS USING NANOSECOND-PULSE PLASMA ACTUATOR

Kentaro Kato
Department of Mechanical Engineering
Keio University
Yokohama 223-8522, Japan
katoken@z3.keio.jp, Kentaro.Kato@aer.mw.tum.de

Christian Breitsamter
Lehrstuhl für Aerodynamik und Strömungsmechanik
Technische Universität München
Boltzmannstr. 15, Garching 85748, Germany
Christian.Breitsamter@aer.mw.tum.de

Shinnosuke Obi
Department of Mechanical Engineering
Keio University
Yokohama 223-8522, Japan
obsn@mech.keio.ac.jp

ABSTRACT

Experimental study was conducted on the flow control over a NACA 65A005 swept wing using a plasma actuation driven by repetitive nanosecond-pulse voltage. The actuator was set near the apex in order to manipulate the leading edge vortices in the post-stall regime. Wind-tunnel tests were conducted for the various angles of attack α at a Reynolds number $Re \equiv C_{\mathrm{m}} U_\infty / \nu = 6.0 \times 10^5$ which was based on the effective chord length C_{m} and freestream velocity U_∞. The actuating frequency f was also varied for 20 Hz $\leq f \leq$ 1000 Hz. The force and moment were obtained as a function of α and f by means of a six axis force sensor. The increase of lift coefficient C_{L} from 0.807 to 0.842 was observed when the actuation was applied at the reduced frequency $F^+ \equiv f C_{\mathrm{m}} / U_\infty \approx 0.86$. The increase of lift coefficient strongly correlated with increase of drag and pitch-up. The frequency dependency of lift increase was affected by α. Also, the frequency dependency was changed if asymmetric actuation on a leading edge was applied. The velocity field in the wake was measured by means of a stereoscopic particle image velocimetry. It was shown that the change in the intensity of streamwise vortex led to the lift enhancement.

INTRODUCTION

Recent attempt to engineering flow control includes advanced technique such as plasma actuators; a dielectric barrier discharge plasma actuator (DBD-PA) driven by repetitive nanosecond(NS)-pulse voltage is one of potential methods. With NS-pulse voltage, the thermal effect of plasma becomes dominant compared with electrohydrodynamic (EHD) effect (Starikovskii *et al.*, 2009). The significant effects on the high-speed flow applications are demonstrated (Sidorenko *et al.*, 2007; Roupassov *et al.*, 2008; Little, 2010; Rethmel *et al.*, 2011; Correale *et al.*, 2011; Hua *et al.*, 2011; Kato *et al.*, 2014). So far, most of works are devoted to control two-dimensional flows.

The aim of the present work is to investigate the effect of NS-pulse-periodic discharge on three-dimensional flows. As a test case, the leading edge vortices (LEVs) on a NACA 65A005 swept wing is selected. Considering related flow instabilities with different time scales, we measure force by means of a force balance for varying repetitive frequency f as well as angle of attack α. For some selected conditions, the wake survey is conducted by means of a stereoscopic particle image velocimetry (stereo-PIV). From the obtained velocity data in the wake, the effects of actuation on the lift and changing vortex structures are investigated.

EXPERIMENTAL METHOD

The entire measurements were carried out in the Göttingen type low-speed wind tunnel facility of the Institute of Aerodynamics and Fluid Mechanics at Technische Universität München.

A full-span NACA 65A005 swept wing model with a chord length of $C|_{y=0} = 315$ mm at the center and a span of $b = 650$ mm was used, cf. Fig. 1. It had a sweep angle of $\Lambda_{25} = 50^\circ$ and an aspect ratio of $AR \approx 2.75$.The model was equipped with pressure taps, through which we measured the surface pressure for baseline case. The Cartesian coordinate system was defined at the apex with the x-axis taken streamwise direction. The y- and z-axes were taken vertical and horizontal direction, respectively.

Plasma actuator consisted of two copper electrodes (3M, 1181: width of exposed and covered electrodes was 6 and 25 mm, respectively. The thickness was 0.07 mm) separated by five layers of 0.07 mm-thick Kapton film (3M, 5413). The length of the electrodes was 200 mm. Actuators were set near the apex, so that the upstream edges of exposed electrodes were located on the leading edges as shown in Fig. 1.

The exposed electrodes were exited by the positive repetitive pulse voltage provided from the power supply (FID GmbH, FPG20-1MC2). It was equipped with two synchronized and independent channels. Each of them nominally provided the voltage pulse with a peak-to-peak voltage $V_{\mathrm{pp}} = 20$ kV under conditions connected with a typical load.

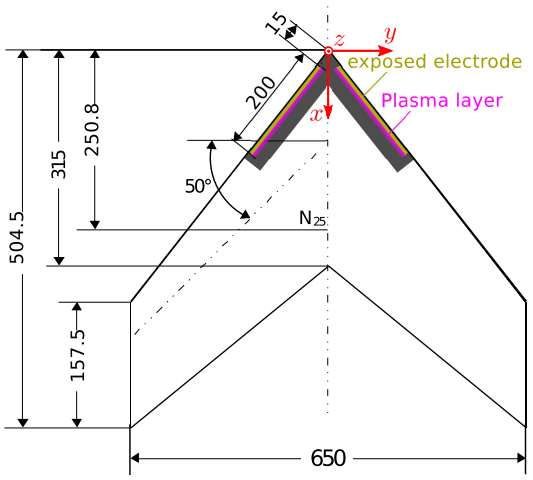

Figure 1. Top-view of the NACA 65A005 wing model

Force Measurement

Force and moment were measured by means of a force balance. The measurement was curried out at a Reynolds number $Re \equiv C_{\mathrm{m}} U_\infty / \nu = 6.0 \times 10^5$ which was based on the effective chord length $C_{\mathrm{m}} \equiv C|_{y=b/4}$ and freestream velocity of $U_\infty \approx 40$ m/s. In addition, in order to address the effect of symmetry, either one channel or two channels were connected to the actuators and effects of actuation on one side and both sides of leading edges were compared.

PIV Measurement

For the case where significant effect of the control on lift coefficient C_{L} was observed ($\alpha = 35^\circ, f = 140$ Hz), the velocity field in the wake was measured by a stereo-PIV system, composed by a Nd:YAG laser and two sCMOS cameras with a resolution of 2560×2160 pixel^2. By comparing two pairs of images of tracer particles taken at constant interval, $\Delta t = 14$ μs, the instantaneous velocity field $\vec{V}(u,\ v,\ w)$ was acquired at two streamwise locations $x/C|_{y=0} = 2.7$ and 3.7. At each location, the wake was resolved by merging 9 measurements with varying horizontal and vertical locations. For each location, 400 samples were acquired at a sampling rate of 12 Hz.

THEORY OF LIFT EVALUATION

In order to consider the contribution of changing vortex structures to C_{L}, C_{L} is estimated based on wake-integral method proposed by Kusunose (2001). Considering control volume that includes the wing model, we estimate the lift coefficient C_{L} as below,

$$C_{\mathrm{L}} \approx \frac{2}{A} \iint_{W_{\mathrm{A}}} \frac{y\omega_{\mathrm{x}}}{U_\infty} \mathrm{d}y\mathrm{d}z - \frac{2}{A} \iint_{W_{\mathrm{A}}} \frac{w(u-U_\infty)}{U_\infty^2} \mathrm{d}y\mathrm{d}z \quad (1)$$

where ω_{x} denotes streamwise vorticity component. W_{A} stands for a control surface that is located downstream of the model and intersects the wake. The first and second terms are related to effects of force exerted by surrounding on the control volume via pressure and momentum flux through control surface, respectively. The obtained values with/without actuation are compared.

RESULTS AND DISCUSSIONS

Baseline

In order to understand basic flow topology, pressure distribution on windward surface and lift curve are discussed. Figure 2 indicate time-averaged surface pressure normalized by dynamic pressure at typical angles of attack α. The negative pressure, or suction on the upper surface due to the leading edge vortex is developed as α increases ($\alpha \leq 20^\circ$). At $\alpha \approx 25^\circ$, the vortex begins to breakdown from the downstream. The breakdown point is propagated to further upstream at higher α and it leads to the gradual stall compared to one on rectangular wings. This is typical behavior of three-dimensional leading edge vortex on swept wings.

The suction peak mainly contributes to the lift generation. The black squares and red circles in Figure 3 show measured C_{L} without actuators (1) and with turned off actuators (2), respectively. The baseline (1) indicates that C_{L} reaches to the maximum $C_{\mathrm{L,\ Max}} \approx 0.97$ at $\alpha \approx 25$–30°. For $\alpha \geq 30^\circ$, C_{L} decreases and it consistents with pressure distribution discussed above.

Lift enhancement

The difference between without actuator (1) and with turned off actuator (2) indicates the passive geometric effect; Mounting actuator changes the thickness and curvature of wing. The blue crossings indicate the typical lift curve with plasma actuation. The active effect of plasma excitation is shown as difference between with turned off actuator (2) and turned on actuator. While the magnitude of active effect is limited, the present work focuses on the active effect.

The active effect has certain systematic trends. Figure 4 shows active effect on increase of the lift coefficient $\Delta C_{\mathrm{L}} = C_{\mathrm{L,\ actuation}} - C_{\mathrm{L,baseline(2)}}$. Whole dataset of ΔC_{L} shows dependency of α and f: For $\alpha = 30^\circ$, a local peak seems to be observed at $f \approx 400$–600 Hz if both leading edges are excited. For $\alpha = 35^\circ$, the actuation on both leading edges provides the maximum increase at $f \approx 140$ Hz (Plot with crossings indicates the same measurement as plot with circles but with finer frequency resolution).

The preference frequency $f \approx 140$ Hz corresponds to $F^+ \equiv f C_{\mathrm{m}} / U_\infty \approx 0.86$. In general, $F^+ = O(0.1)$ is known as characteristic frequency associated with vortex shedding (Gursul *et al.*, 2007). On the other hand, the preference range $f \approx$ 400–600 Hz corresponds to $F^+ \approx 2.45$–3.68. $F^+ = O(1)$ is typical frequency range associated with helical mode instability (Gursul *et al.*, 2007).

As the effect of symmetry on the control authority, ΔC_{L} with actuation on one and both sides of the leading edges at $\alpha = 35^\circ$ are compared in Fig. 4. Although only half of input energy was applied for actuation on one side compared with on both sides, ΔC_L with actuation on one side becomes comparable to that on both sides at higher f. It can imply that asymmetric excitation, e.g., actuation on both leading edges with opposite phases, works more effectively to manipulate the helical mode instability.

As the further analysis, increases of all six components due to the actuation on both leading edges are shown in Figure 5–10. They indicate that the lift increase shown in Figure 4 correlates strongly with increase of drag and pitch-up. In contrast, no significant correlation with ΔC_{L} and rolling moment is observed. The same trend was observed for the case with only one side actuation although whole mappings

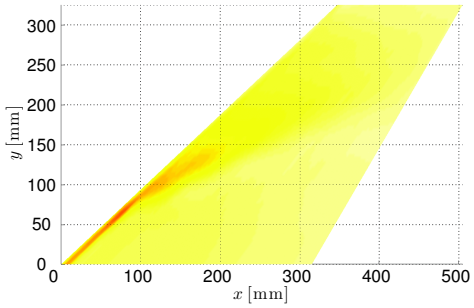

(a) $\alpha = 8°$

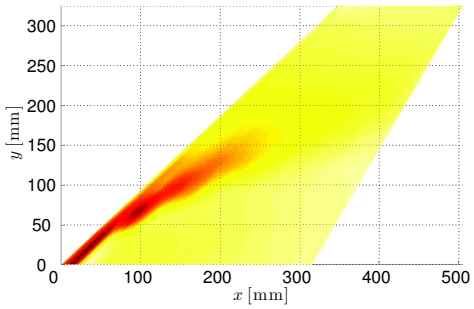

(b) $\alpha = 15°$

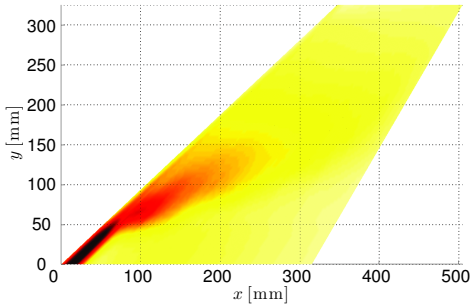

(c) $\alpha = 20°$

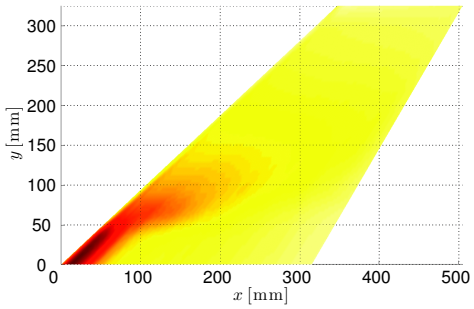

(d) $\alpha = 25°$

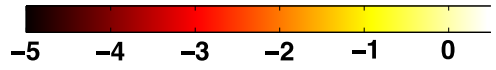

Figure 2. Averaged pressure coefficient $\overline{C_p}$ on upper surface at typical angles of attack α

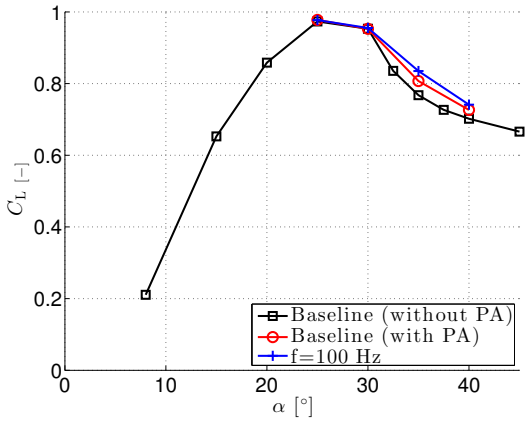

Figure 3. Lift curve

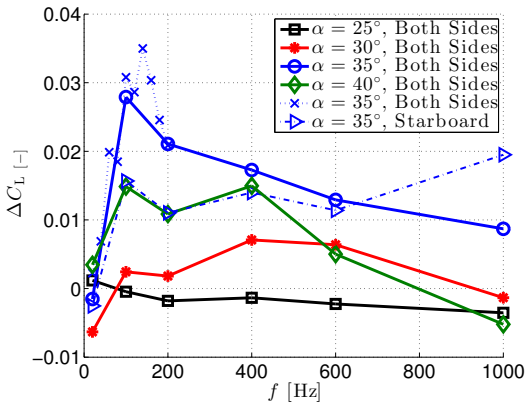

Figure 4. Increase of lift coefficient due to plasma actuation

of increase of coefficients are not repeated here.

This correlation among increase of lift, drag and pitching moment coefficients can be explained as induced drag and changing pressure near the apex. Because the increase of lift accompanies significant increase of pitching moment but not rolling moment even with one side actuation, change of pressure at a inboard location with certain distance from the support can be considered. The recovery of suction peak near the apex is a plausible scenario to explain the increase of lift and correlations with other force/moment components.

Compared with lift enhancement in two-dimensional separation control on rectangular wings (Sidorenko *et al.*, 2007; Roupassov *et al.*, 2008; Little, 2010; Rethmel *et al.*, 2011; Correale *et al.*, 2011; Hua *et al.*, 2011; Kato *et al.*, 2014), effects on lift on the swept wing are quite different. First, no effect due to promoting transition from laminar to turbulent on lift enhancement is observed near the stall regime; The active trip brings no impact because the transition on swept wings occurs naturally much earlier. Second, the impact of the aforementioned effect in the post-stall regime is limited; The increase of lift coefficient in the present work is one order of magnitude smaller than that in typical two-dimensional flow controls on on rectangular wings (Sidorenko *et al.*, 2007; Roupassov *et al.*, 2008; Little, 2010; Rethmel *et al.*, 2011; Correale *et al.*, 2011; Hua *et al.*, 2011; Kato *et al.*, 2014).

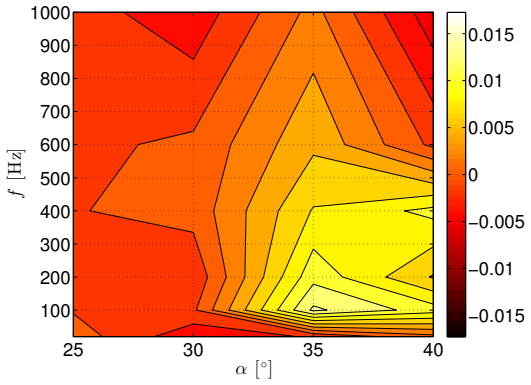

Figure 5. Increase of drag coefficient ΔC_{D}

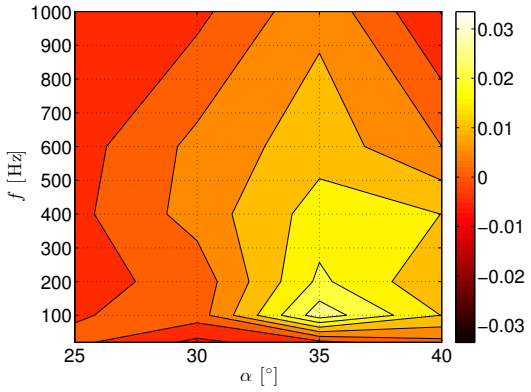

Figure 6. Increase of lift coefficient ΔC_{L}

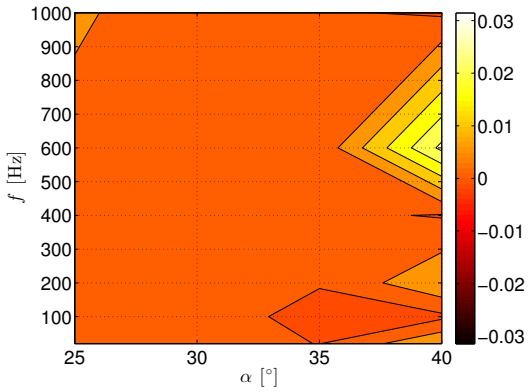

Figure 7. Increase of lateral force coefficient ΔC_{Q}

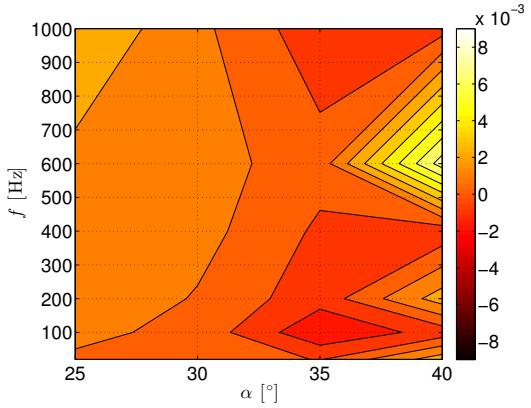

Figure 8. Increase of rolling moment coefficient ΔC_{Mx}

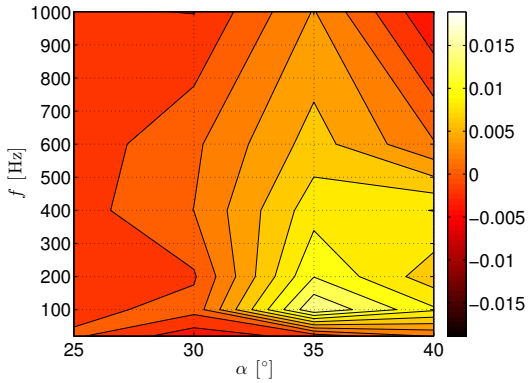

Figure 9. Increase of pitching moment coefficient ΔC_{My}

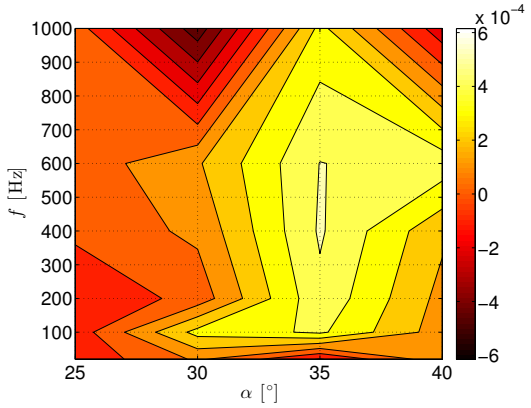

Figure 10. Increase of yawing moment coefficient ΔC_{Mz}

Flow structures in the wake

As the detailed information to ensure the active effect and to access the vortex structure, PIV measurement was conducted. The result shows vortex structures in the wake. Color contour and lines in Fig. 11 (a) indicate time-averaged streamwise vorticity ω_{x} and streamline at $x/C|_{y=0} = 2.7$ for actuated case, respectively. On the inboard section ($|y/b|$ ≈0.05–0.34), dominant counter-rotating LEVs are located. Around wing tips ($|y/b|$ ≈0.5), wing tip vortices, which are rotated in the same direction as the LEVs, are generated and merged into LEVs. Below the LEVs (y/b ≈0.29–0.42), vortices rotated in the opposite direction to the LEVs exist.

Integral analysis

C_{L} measured by force balance and estimated based on wake-integral method are summarized in Table 1. C_{L} estimated from $\vec{V}$ at two locations is underestimated for both baseline and controlled cases. However, the active effect of plasma ΔC_{L} is still observable.

The spanwise distributions of the first (solid lines) and second (dashed-dotted lines) terms in Eq. (1) are shown in Fig. 11 (b). Black and red lines indicate cases without/with

Table 1. Lift coefficient obtained by means of force balance and integral analysis

	Balance	Wake survey	
$x/C\|_{y=0}$	-	2.7	3.7
$C_{\mathrm{L,\ off}}$	0.807	0.7433	0.7098
$C_{\mathrm{L,\ on}}$	0.842	0.7694	0.7313
ΔC_{L}	0.035	0.0261	0.0215

actuation, respectively. The first term mainly contributes to the lift. For the first term, the positive and negative effects of actuation are observed at $|y/b| \approx 0.21$–0.37 and 0.37–0.49, respectively. This positive effect on lift generation is caused by intensified streamwise vorticity in LEVs.

Thus, these measurements of force and velocity field in the wake revealed that the plasma actuation changed the intensity of streamwise vorticity in LEVs and surface pressure near the apex, where LEVs originate. Although the magnitude of lift increase is small relative to one in typical separation control on rectangular wings (Sidorenko *et al.*, 2007; Roupassov *et al.*, 2008; Little, 2010; Rethmel *et al.*, 2011; Correale *et al.*, 2011; Hua *et al.*, 2011; Kato *et al.*, 2014), these measurements showed lift enhancement due to the manipulation of LEVs.

CONCLUSIONS

Flow control over a NACA 65A005 swept wing using plasma actuation driven by repetitive nanosecond-pulse voltage was experimentally investigated. The actuation was applied near the apex, so that the leading edge vortices were manipulated and the lift was recovered in the post-stall regime. The force was measured by means of a force balance at a Reynolds number $Re \equiv C_{\mathrm{m}} U_\infty / \nu = 6.0 \times 10^5$ which was based on the effective chord length and freestream velocity. The effect was evaluated in the range of angle of attack $25^\circ \leq \alpha \leq 40^\circ$ and actuation frequency 20 Hz$\leq f \leq$1000 Hz.

The largest increase of lift coefficient C_{L} from 0.807 to 0.842 was observed at $\alpha = 35^\circ$ when the actuation was applied at the reduced frequency $F^+ \equiv f C_{\mathrm{m}} / U_\infty \approx 0.86$. The frequency dependency of lift increase was affected by α. Also, the frequency dependency was changed if asymmetric actuation on one leading edge was applied. It was also found that the lift increase correlated strongly with increase of drag and pitch-up but not with rolling moment for both actuations on one and two leading edges. These correlations indicate that the actuation affects suction pressure near apex, where LEVs originate. In order to investigate the effect of the actuator on the vortex structure, the velocity field in the wake was measured by means of a stereoscopic particle image velocimetry. The velocity data showed the intensified streamwise vorticity in LEVs led to the lift enhancement.

ACKNOWLEDGEMENTS

This work was supported by Erasmus Mundus action 2 project "BEAM Build on Euro Asian Mobility" and also was achieved as an international internship program for COE Research Assistant of Keio University Global Center of Excellence Program "Center for Education and Research of Symbiotic, Safe and Secure System Design". We appreciate the offers of electric devices from FID GmbH. We would like to thank Dr. Y. Oyamada at Tottori University for the suggestion related to pressure measurement. We express also our gratitude to Janik Kiefer for contribution to the measurements.

REFERENCES

Correale, G., Popov, I., Nikipelov, A., Pancheshnyi, S., Starikovskii, A.Y., Hulshoff, SJ & Veldhuis, LLM 2011 Experimental study and numerical simulation of flow separation control with pulsed nanosecond discharge actuator. *Bulletin of the American Physical Society* **56**.

Gursul, I., Wang, Z. & Vardaki, E. 2007 Review of flow control mechanisms of leading-edge vortices. *Progress in Aerospace Sciences* **43** (7-8), 246–270.

Hua, L., Shangen, C., Shengzhi, Z. & Junxing, B. 2011 Experimental investigation of airfoil suction side flow separation control by spanwise nanosecond actuation. In *Measuring Technology and Mechatronics Automation (ICMTMA), 2011 Third International Conference on*, , vol. 2, pp. 108–111. IEEE.

Kato, K., Breitsamter, C. & Obi, S. 2014 Flow separation control over a gö 387 airfoil by nanosecond pulse-periodic discharge. *Experiments in Fluids* **55** (8), 1795.

Kusunose, Kazuhiro 2001 Lift analysis based on a wake-integral method. In *39th AIAA Aerospace Sciences Meeting & Exhibit, Reno, Nevada, AIAA-2001-0420*.

Little, J. C. 2010 High-lift airfoil separation control with dielectric barrier discharge plasma actuators. PhD thesis, The Ohio State University.

Rethmel, C., Little, J., Takashima, K., Sinha, A., Adamovich, I. & Samimy, M. 2011 Flow separation control over an airfoil with nanosecond pulse driven dbd plasma actuators. *AIAA Paper* (2011-0487).

Roupassov, DV, Nikipelov, AA, Nudnova, MM & Starikovskii, A.Y. 2008 Flow separation control by plasma actuator with nanosecond pulse periodic discharge. In *Gas Discharges and Their Applications, 2008. GD 2008. 17th International Conference on*, pp. 609–612. IEEE.

Sidorenko, A., Zanin, B., Postnikov, B., Budovsky, A., Starikovskii, A., Roupassov, D., Zavialov, I., Malmuth, N., Smereczniak, P. & Silkey, J. 2007 Pulsed discharge actuators for rectangular wing separation control. *AIAA Paper* (2007-941).

Starikovskii, A.Y., Nikipelov, A.A., Nudnova, M.M. & Roupassov, D.V. 2009 Sdbd plasma actuator with nanosecond pulse-periodic discharge. *Plasma Sources Science and Technology* **18**, 034015.

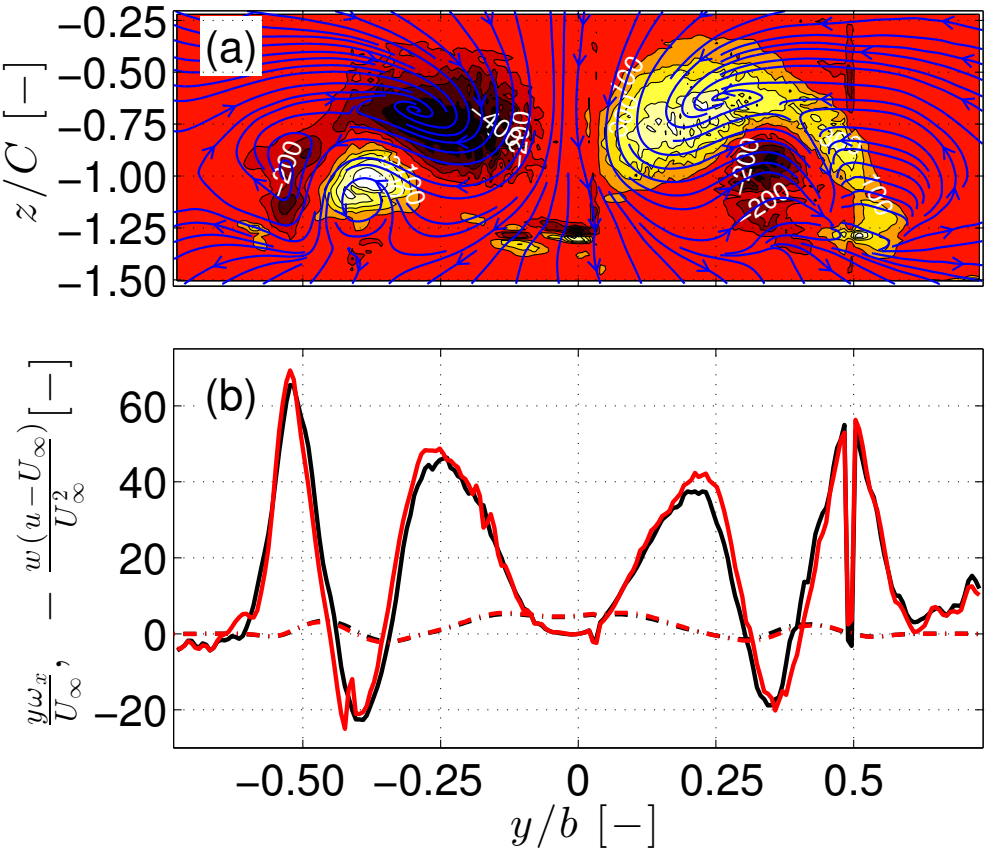

Figure 11. Vortex structures in the wake and the contribution to the lift: (a) time-averaged streamline and streamwise vorticity component. (b) Spanwise distribution of the first (solid lines) and second (dashed-dotted lines) terms in Eq. (1). Black and red lines indicate values without/with actuation, respectively.